

7th CIRP Conference on Surface Integrity

Stream Finishing of Additively Manufactured AlSi10Mg PBF-LB Parts: Influence on Surface Quality and Fatigue Behaviour

Helena Wexel^{*a}, Steffen Kramer^{a,b}, Johannes Schubert^a, Volker Schulze^a, Frederik Zanger^a^a*wbk Institute of Production Science, Karlsruhe Institute of Technology, Kaiserstr. 12, 76131 Karlsruhe, Germany*^b*IFSW Institut für Strahlwerkzeuge, University of Stuttgart, Pfaffenwaldring 43, 70569 Stuttgart, Germany*^{*} Corresponding author. Tel.: +49 1523 9502637; fax: +49 721 608-45005. E-mail address: helena.wexel@kit.edu

Abstract

Due to the large design freedom of additive manufacturing (AM), components manufactured by laser powder bed fusion (PBF-LB) possess a high lightweight potential, which increases the importance of PBF-LB for applications in the automotive, aviation and aerospace industries. The typically high surface roughness of PBF-LB parts leads to a significant reduction in fatigue strength. Therefore, a finishing process for improving the surface roughness of complex PBF-LB parts is required. Stream finishing represents such a process. In a first step, surface roughness evolution and abrasion rates were measured for specimens manufactured with PBF-LB at different stages of the finishing process. In a second step, fatigue specimens were manufactured, machined both by turning and stream finishing, and tested by rotating bending fatigue tests. To evaluate crack initiation and propagation, the fracture surfaces were examined by scanning electron microscopy. The microstructure and microhardness near the surface were investigated to assess the influence of the surface layer on the fatigue behaviour. Stream finishing proved to be a suitable finishing process, as the specimens exhibited very low surface roughness and improved fatigue behaviour compared to turned specimens, especially for lower stresses.

© 2024 The Authors. Published by Elsevier B.V.

This is an open access article under the CC BY-NC-ND license (<https://creativecommons.org/licenses/by-nc-nd/4.0>)

Peer-review under responsibility of the scientific committee of the 7th CIRP Conference on Surface Integrity

Keywords: Additive Manufacturing; Laser Powder Bed Fusion; Finishing; Fatigue Strength, Surface modification, AlSi10Mg

1. Introduction

Over the past decade, the additive manufacturing industry has become increasingly important and additive manufacturing processes are already a reality in industrial production [1]. In addition to the pure prototyping and design phase, load-bearing and safety-relevant components as well as complete products are manufactured [2]. The focus is on topology optimisation, function integration and resource conservation [3]. In this context, additive manufacturing has emerged as the preferred technology because of its ability to define complex shapes with internal geometries [4]. Laser powder bed fusion (PBF-LB) is one of the most widely used additive manufacturing processes. The ability to manufacture near-net-shape components enables efficient and resource-saving use of materials and reduces the need for further manufacturing steps and additional machine

tools [5]. According to Aboulkhair et al. [6], PBF-LB of aluminium alloys is of great research interest for high value manufacturing applications in the aerospace and automotive industries. However, in order to demonstrate the reliability of additively manufactured aluminium components, their mechanical properties must first be fully investigated [6]. Previous studies such as Yang et al. [7] have shown that the static mechanical properties achievable by the PBF-LB process exceed those of conventional processes. However, particularly in the field of mechanical engineering, the fatigue strength of materials and structures is usually more important than the static strength [8]. Yet, according to Sausto et al. [9] the disadvantages of additively manufactured alloys have so far limited their application to load-bearing components. For example, the formation of internal defects, low surface quality and detrimental residual tensile stresses are unavoidable with

laser powder bed fusion [9]. Richard et al. [2] state that additively manufactured components generally achieve lower fatigue strength than conventionally manufactured components due to process-related defects in the material. In particular, fatigue properties of additively manufactured components are influenced by surface finish, internal defects, microstructure and residual stresses [2]. These characteristics are ranked in order of influence: Surface roughness has the greatest influence on fatigue strength and internal irregularities are more critical than effects of microstructure [10, 11, 12]. Consequently, the typically high surface roughness of PBF-LB components leads to a significant reduction in fatigue strength. However, the often complex geometry of additive components makes surface finishing difficult. Therefore, stream finishing as a post-processing method to improve surface roughness especially of complex PBF-LB components offers a promising solution. According to Schulze et al. [13], in contrast to classical shot peening, the stream finishing process not only reduces surface roughness but also allows a defined induction of residual compressive stresses. Compared to vibratory finishing, stream finishing results in higher relative flow speeds between workpiece and abrasive, resulting in high surface quality with reduced machining time and thus increased productivity [13]. Furthermore, the ability to control the alignment of the components allows optimum adjustment of the applied forces and material removal [14]. Previous stream finishing studies have primarily focused on the qualification of the surface modification process [13, 14, 15]. Optimal process times for AISI4140 plane specimens have already been investigated [13], the influence of rotational speed on surface states has been considered [15] and the process has been optimised by numerical and experimental process analysis [14]. However, the processing of additively manufactured specimens in stream finishing has not yet been investigated, with the large deviation of the initial surface from investigations of previous work necessitating a separate investigation. Therefore, the aim of this study is to explore the potential of the stream finishing process for post-processing of additive load bearing component and due to the importance of fatigue behaviour for applications particularly in the field of mechanical engineering, the influence of the stream finishing process on cyclic strength will also be investigated as a further objective.

In a first step, surface roughness evolution as well as the abrasion rate of PBF-LB manufactured specimens at different stages of the finishing process were analysed. In a second step, additively manufactured fatigue specimens were post-processed by stream finishing and investigated in the rotating bending fatigue test. The results were compared with those of specimens with a turned and as-built surface. To evaluate crack initiation and propagation, fracture surfaces were analysed using a scanning electron microscope.

2. Materials and Methods

AlSi10Mg powder supplied by m4p material solutions GmbH with a particle size distribution of 20-63 μm was used to produce PBF-LB components of the specimens considered in this work. The specimens were manufactured perpendicular to the build platform on an SLM280HL machine with qualified

process parameters to achieve part densities $> 99.7\%$. The layer thickness was 50 μm and the focus diameter 80 μm . Laser power was 350 W, scan speed was 1150 mm/s and hatch offset was 0.17 mm. The platform was preheated to 100°C and the scan rotation per layer was 67°. The specimens were separated from the build platform using electrical discharge machining (EDM).

The final geometry of the specimens after finishing is based on DIN 50113 and can be seen in Fig. 1. According to the standard, the ratio of the clamping cross section A_c to the test cross section A is approximately 2.6, which is within the recommended range for brittle materials. The turned specimens were machined on a Weiler E30 machine, using D-inserts with a 55° wedge angle, a clearance angle of 6° - 8° and a cutting edge radius of 0.4 mm. The specimens were clamped between centres and machined with a cutting speed of 80 m/min. The feed rate for roughing was 0.1 mm/rev. and 0.07 mm/rev. for finishing, respectively. A schematic view of the stream finishing machine is shown in Fig. 2. For stream finishing the machine SF1 68 (Otec Präzisionsfinish GmbH) was used. The grinding media was a high density sintered aluminium oxide ceramic (KXMA 16) with an average grain size of 1.7 mm to 2.4 mm, wetted with water and compound. The qualified process parameters used are listed in Table 1. To ensure linear removal over the length of the specimen, the specimens were flipped after each time interval. To analyse abrasion rates and surface roughness evolution, three additional specimens were tested in advance at increasing time intervals. The specimens were cleaned for three minutes in an ultrasonic bath. The mass change was determined using a Mettler Toledo B204-S balance. The 3D confocal measuring system Nanofocus μsurf custom was used to determine surface roughness evolution. An Olympus lens with 20x magnification and an area coverage of 800 μm x 800 μm at a working distance of 12 mm was used for the measurements.

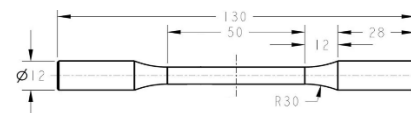


Fig. 1. Final geometry specimen, dimensions in mm.

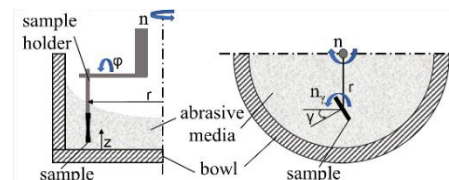


Fig. 2. Schematic view of the stream finishing machine [14].

Table 1. Process parameters stream finishing.

Parameter	Symbol	Value
Depth of immersion	z	150 mm
Radius of immersion	r	250 mm
Angle of immersion	φ	0°
Rotational speed of the specimen	n_s	10 min^{-1}
Rotational speed of the bowl	n	70 min^{-1}

To ensure coaxial clamping during the rotating bending fatigue test, the clamping surfaces of the stream-finished and as-built specimens were turned. As mentioned above, the fatigue properties of additively manufactured components are mainly influenced by surface finish and internal defects. Therefore, an optical porosity analysis of six specimens and a surface roughness analysis of all specimens following fabrication and post-processing were performed.

The cyclic behaviour of the specimens was evaluated using rotating bending fatigue test according to DIN 50113:2018-12. Loading a rotating specimen with a constant bending moment results in a mean stress $\sigma_m = 0$ MPa or a stress ratio R of -1, giving the bending fatigue strength σ_f .

To determine the Wöhler curve in the high cycle fatigue (HCF) range, several tests at different loads were conducted by the pearl string method according to standard DIN 50100:2021-09, which is recommended for an initial assessment of fatigue behavior. A data point was considered to be a run-out when the number of load cycles was $> 1E7$. The mean value and slope of the Wöhler curve were determined at a failure probability of 50 % according to the following equation:

$$N = C * \sigma_a^{-k} \quad (1)$$

where C is the intercept and k the slope of the Wöhler curve and σ_a is the stress amplitude.

The fractography images of all fracture surfaces were taken with a JEOL JSM-6010 LV SEM. To evaluate the cold working effect of the stream finishing process, the Vickers microhardness (HV 0.1) of the stream-finished specimens was measured using the Qness Q10A+ hardness testing system in accordance with DIN EN ISO 6507. The microhardness in the centre of the specimen and the microhardness at a distance of 120 μm from the edge of the specimen were examined. For every specimen type, two samples were measured with five measurement points in the edge and central areas each.

3. Results

The results of the roughness change and mass abrasion during stream finishing as a function of machining time are shown in Fig. 3. The surfaces of the stream finished specimens were measured at three different positions and an average value for S_a was calculated. The selected drum speed of 70 min^{-1} results in a significant surface improvement from $S_a \approx 10 \mu\text{m}$ to $S_a \approx 0.3 \mu\text{m}$, which remains constant even at longer processing times. Hashimoto et al. [16] have developed the fundamentals for predicting surface roughness in vibratory finishing and defined a suitable mathematical model, which will be validated in the following as a formal means for characterising stream finishing of specimens with additive as-built surfaces. According to Schulze et al. [13], the removal mechanisms of roughness change and micro cutting in vibratory finishing can also be applied to stream finishing of conventionally manufactured components. The surface roughness reaches a saturation value after a certain machining time and as stream finishing continues, the mass difference Δm increase [13]. The separation can also be observed in the stream

finishing of additively manufactured specimens and can be defined according to Fig. 3 at a processing time of $t \approx 220$ minutes. After this processing time the roughness value S_a reaches the saturation value of $S_a \approx 0.32 \mu\text{m}$, while the accumulated mass difference shows a linear course. The results are in agreement with the observations of [16]. Accordingly, the mathematical model for predicting surface roughness during vibratory finishing according to equation (2) by Schulze et al. [13] is applied to the curve fitting of the average roughness value S_a of the stream finished specimens. The roughness value S_a is formulated as a function of the grinding time t . S_{a0} describes the initial value and $S_{a\infty}$ the saturation value of the roughness. The parameter A is obtained, according to the fit, as $A = 0.024 \text{ min}^{-1}$. The resulting curve fit shows an adequate fit ($R^2 = 0,94$).

$$S_a(t) = (S_{a0} - S_{a\infty}) * \exp(-A * t) + S_{a\infty} \quad (2)$$

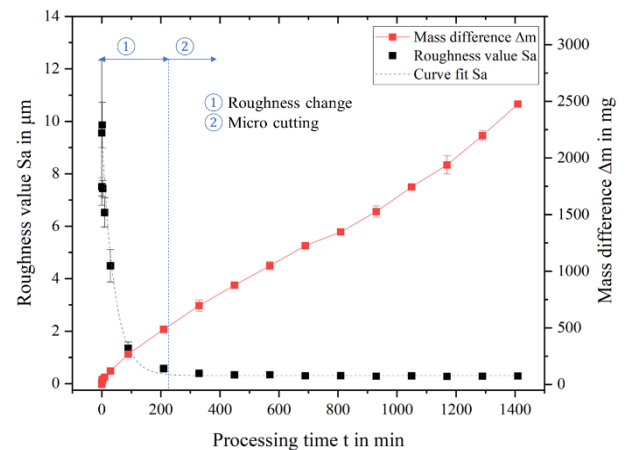


Fig. 3. Roughness and mass difference vs. processing time.

The forces applied during the stream finishing process have been investigated by [14] from which a bending stress of approximately 10 MPa can be conservatively estimated in this case. The load during the process is therefore negligible in terms of cyclic fatigue strength. However, it cannot be excluded that the stream finished specimens may have exhibited a slight curvature as a result of the pre-processing steps, such as the fabrication of the threaded holes for fixation during stream finishing.

Fig. 4 shows the successive changes in the surface profile based on a representative 3D view after each time interval. Initially, process-induced micro-roughnesses, which depend on melting energy, powder particle size distribution and layer thickness [17], are smoothed out, resulting in a dented surface. After $\Delta t = 60$ min, these dents are clearly flattened which results in a wavy surface, with a structure too large to be represented by the section considered ($0.8 \times 0.8 \text{ mm}^2$). After a total processing time of $t = 360$ min, the dented structure is completely removed. From the results of the abrasion curve and surface roughness development (Fig. 3), an optimum process time of 360 min with a rotation of the specimen after 180 min for homogeneous processing results was selected to process the fatigue specimens.

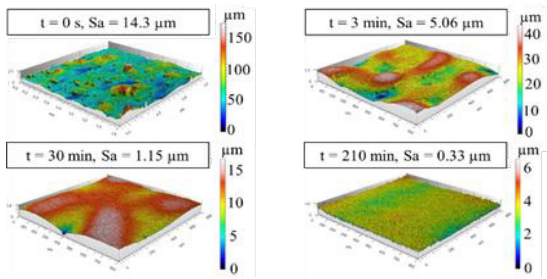


Fig. 4. Representative 3D views of the surface measurement.

With a mean value of $\rho = 99.75\%$ and a standard deviation $SD = 0.08\%$, the optical porosity analysis showed expected relative densities of additively manufactured specimens. Moreover, the density is similar for all specimen types and should only be considered as a general information, but is not relevant for the interpretation of the different fatigue behaviours. In order to be able to relate the effect of the surface finish to the results of the rotating bending fatigue test, the mean values and SD's of the roughness value S_a for all specimens are determined from three measurements per specimen. For the as-built specimens, $S_a = 14.02\ \mu\text{m}$ with $SD = 2.11\ \mu\text{m}$. SD values are relatively high, partly because of the poor reproducibility caused by the additive manufacturing, and partly because both optical and tactile measuring systems are limited by the high surface roughness caused, for example, by powder sintering [18]. The best measurement result of $S_a = 0.32\ \mu\text{m}$, with $SD = 0.02\ \mu\text{m}$, is provided by the stream finished specimens. For the turned specimens, the S_a value is $S_a = 1.15\ \mu\text{m}$ with $SD = 0.06\ \mu\text{m}$. The mean and SD of the microhardness of the different specimens are given in Table 2, depending on their distance from the specimen surface.

Table 2. Mean value and SD of microhardness depending on surface distance.

Specimen	Specimen centre		120 μm	
	HV0.1	SD	HV0.1	SD
as-built	136.3	4.6	131.3	3.5
turned	141.4	4.5	138.6	4.7
stream finished	137.3	4.1	135.2	4.1

Fig. 5 shows the data points of the rotating bending fatigue test as well as the determined Wöhler curves of the as-built, the turned and the stream-finished specimens. The inclination of the Wöhler lines k is $k = 4.34$ for the as-built specimens, $k = 6.67$ for the turned specimens and $k = 16.57$ for the stream-finished specimens. A comparison of the determined Wöhler curves of the as-built specimens also shows a downward shift of the curve of the turned specimens. The data point for the stream-finished specimen set at a stress amplitude of 60 MPa was not included in the determination of the Wöhler curves according to VDI 3405-2 and was marked as "not evaluated". The Wöhler curve of the stream-finished specimens is significantly flatter. In the range of high cycle numbers, the stream-finished specimens show a higher fatigue strength than the turned specimens. However, at cycle numbers below $1E5$, the data points of the stream-finished specimens are below those of the turned specimens.

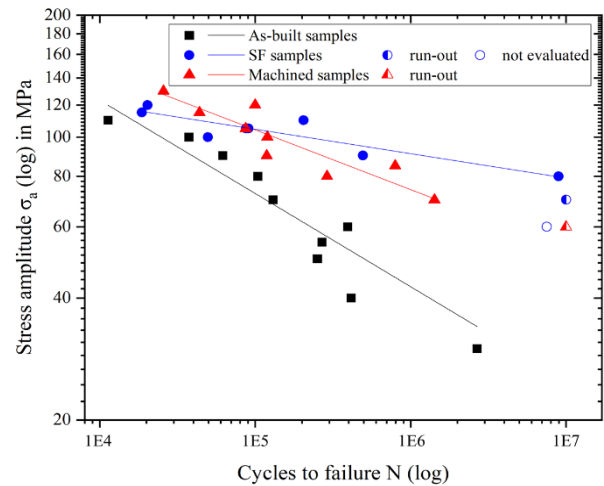


Fig. 5. Wöhler curves of AlSi10Mg specimens.

In the course of the fractographic investigations, both the ratio of fatigue fracture area to total fracture area and the cause of crack initiation and crack propagation are of interest. In combination with the determined sections of the Wöhler curves, a closer look at these factors provides insight into the behaviour of additively manufactured AlSi10Mg specimens with differently modified surfaces. Fig. 6 shows exemplary SEM images of the total fracture area and the crack initiation location of the different sets of specimens for specimens that have undergone a number of load cycles around $N \approx 1E6$. The ratio of the fatigue fracture area to the total fracture area R_A in this case is $R_A = 15.67\%$ for the as-built specimen, $R_A = 64.97\%$ for the turned specimen and $R_A = 28.23\%$ for the stream-finished specimen. For the as-built specimen it can be seen that the crack initiation started from an irregularity in the surface. A pore at the surface for turned specimens or near the surface for stream finished specimens can be identified as the cause of the crack initiation.

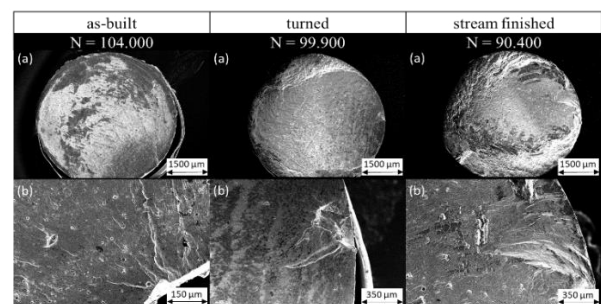


Fig. 6. Exemplary SEM images of the fracture surfaces: (a) total fracture surface; (b) cause of crack initiation.

4. Discussion

The surface roughness analysis showed that stream finishing of additive specimens resulted in a significant reduction in surface roughness, even lower than that of turned specimens, and is therefore suitable as a surface finishing process. Analogously to vibratory finishing, two different removal mechanisms could be defined: roughness change and micro-cutting. For additive specimens, the transition occurred at a process time of approximately 180 minutes.

The results of the rotating bending fatigue test illustrate the dominant influence of surface finish on cyclic strength. Surface optimization resulted in an upward shift and flattening of the Wöhler curve in the fatigue strength range.

The as-built specimens achieved a significantly lower fatigue strength than the stream finished and turned specimens with a lower Sa value, shown by the steeper slope and the downward displacement along the stress amplitude. Higher surface roughness thus resulted in a steeper Wöhler curve with a lower stress amplitude.

Hardness measurements showed a decrease in hardness from the centre of the specimen to the outer layer. The decrease in hardness for the as-built specimens was caused by the chosen contour scanning strategy. Microscopic examinations of the near-surface microstructure confirmed the location of the hardness measurements near the edge still being within the contour run of the scanning strategy for the as-built specimens. The lower cooling rate of the selected contour parameters (laser power 250 W, scan speed 555 mm/s, laser focus offset -4 mm) resulted in a ductile surface layer with reduced hardness.

According to Radaji and Vormwald, the ratio of the size of the residual fracture surface to fatigue fracture surface provides an indication of the applied load [19]. Fractographic studies of the as-built specimens showed that the ratio of fatigue fracture area to residual fracture area decreased with increasing load. The fatigue fracture area of the as-built specimens was small compared to the other specimen types, despite lower loads were applied. This can be explained by the fact that in the rotating bending fatigue test the highest load was applied to the edge of the specimen. For as-built specimens, the surface was subject to numerous stress peaks caused by the high surface roughness and tensile residual stresses due to the PBF process. This accelerated crack propagation, especially along the specimen edge, resulting in the characteristic semi-circular fatigue fracture area shown in Fig. 6. Surface roughness contributed to an increase in the number of crack initiation sites on the surface of the specimen, reducing fatigue life through earlier crack initiation and faster propagation rates due to higher driving forces resulting from the increased number of surface cracks.

Turned specimens with lower Sa values achieved higher fatigue strength than the as-built specimens, as indicated by the flatter slope at a higher stress amplitude of the Wöhler curve.

The results showed an overall higher hardness for the turned specimen. This can be attributed to the location of the measured specimen section, which was at the top of the vertically printed specimen and therefore, was less influenced by the preheating temperature of the build platform. The mean values of the turned specimens showed a slight decrease in hardness from the centre of the specimen to the outer layer. During turning, a high load can lead to thermomechanical stress and thus, to a change in microstructure [20]. This provides an explanation for the reduced hardness in the edge region of the turned specimen. However, it should be noted that the difference in hardness was relatively small compared to the high SD.

The ratio of fatigue fracture area to residual fracture area of the turned specimens decreased with increasing load, confirming the results of the fracture surface analysis, providing an indication of the applied load.

The fatigue fracture area of the turned specimens was larger compared to the as-built specimen, since the lower surface roughness caused crack initiation to occur later. Scanning electron microscope (SEM) investigations of the turned specimens showed that the causes of crack initiation were consistently near or at the surface and were often an irregularly shaped oxide or lack of fusion pores. These pores, originally in the interior of the specimen, have been uncovered to or near the surface by turning. Accordingly, despite a high relative density, the residual porosity from the manufacturing process in the form of a critical defect near or at the surface was sufficient to cause fatigue failure.

Overall, the HCF strength results for stream finished specimens can be compared to those of turned specimens. In the range of high load cycles above $1E5$, a clear improvement in cyclic behaviour could be observed due to the lower slope of the Wöhler curve.

It should be noted, that the possible slight curvature resulting from the pre-processing steps may have resulted in superimposed stress states during the rotating bending fatigue test, primarily affecting the stress at the specimen edge and thus, counteracting the effect of the stream finishing process.

The mean values of the stream finished specimens also showed a slight decrease in hardness from the centre of the specimen to the outer layer. Similarly, to the as-built specimens, the hardness measurement near the edge was still within the contour run of the scanning strategy, but the decrease in hardness was less, compared to the as-built specimen, possibly due to the stream finishing process. Again, it has to be noted, that the difference in hardness was relatively small compared to the high SD.

Based on the results from the literature, it is assumed that the stream finishing process induced residual compressive stresses close to the surface: Schulze et al. [13] recorded significant residual compressive stresses as a result of cold deformation in the near-surface region for conventionally manufactured specimens of AISI4140 using the stream finishing process. Bagherifard et al. [21], investigated the influence of shot peening on the fatigue strength of additively manufactured AlSi10Mg specimens, resulting in compressive residual stresses up to 400 μm penetration depth and a significant increase in hardness in the surface layer for less than 150 μm [21].

Therefore, it can be assumed that stream finishing also introduced residual compressive stresses in the edge region of AlSi10Mg parts manufactured by PBF-LB. In this case, induced residual compressive stresses would have the same effect on the shape and slope of the Wöhler curve as reduced surface roughness [2]. However, further research is required to confirm this assumption.

As already observed for as-built and turned specimens, the fracture surface provided an indication of the applied load, with the ratio of fatigue fracture area to residual fracture area of the stream finished specimens decreasing with increasing load.

The analysis of the fracture surfaces showed that crack initiation in the stream-finished specimens occurred mainly at an internal oxide or lack of fusion pore near the surface. This observation indicates that the pores were uncovered to the surface by material removal are closed again during the stream

finishing process. The displacement of the crack initiation to a subsurface layer resulted in an atypical fracture surface characterised by the sickle-shaped formation of the stress fracture surface (Fig. 6). Similar observations were made by Bagherifard et al. [21] who termed this effect "fisheye crack". This atypical sickle-shaped stress fracture surface also occurred in a weakened form at the turned samples. It can be assumed that, due to the lower ductility and the lack of residual compressive stresses, crack propagation progressed more rapidly in turned specimens than in stream-finished specimens, resulting in a comparatively larger fatigue fracture area.

As noted above, the crack initiating defects in both the stream finished and turned specimens were lack of fusion or oxide pores. Since the critical defect for failure was similar in both cases, it is likely that further reduction in surface roughness due to stream finishing is not the decisive factor contributing to the flattening of the Wöhler curve of the stream finished specimens, but rather the closing of pores, delaying crack initiation and presumably the introduction of residual compressive stresses and slowing down crack propagation. This also explains why the determined fatigue fracture surfaces of the stream finished specimens were even smaller compared to the fatigue fracture surfaces of the turned specimens.

5. Conclusion

In this work AlSi10Mg specimens were manufactured by laser powder bed fusion. The potential of the stream finishing post-process to reduce surface roughness and increase the HCF strength of complex component geometry for lightweight applications was investigated. Based on the results obtained, the following main conclusions can be drawn:

- Stream finishing of additively manufactured specimens with a roughness value of $S_a = 0.32 \mu\text{m}$ achieves a greater increase in surface quality than turning ($S_a = 1,15 \mu\text{m}$) and is therefore suitable as a surface finishing process.
- Fatigue strength can be significantly increased compared to the as-built specimens. The closing of pores and the presumed introduction of compressive residual stresses during stream finishing, combined with reduced surface roughness, results in a flat Wöhler curve which at high load cycles is well above the Wöhler curve of turned specimens. However, further research is required to confirm the introduction of compressive residual stresses.

In conclusion, stream finishing of complex additively manufactured specimens has great potential to significantly reduce surface roughness and improve fatigue behaviour, especially at high load cycles.

Acknowledgements

The presented work was funded by the Ministry of Science, Research and the Arts of the Federal State of Baden-Wuerttemberg within the 'InnovationCampus Future Mobility', which is gratefully acknowledged. The authors declare no conflict of interests in this work.

References

- [1] Marquardt, E. (2020). 3D-Druckverfahren sind Realität in der industriellen Fertigung. *Zeitschrift für wirtschaftlichen Fabrikbetrieb*, 115(7-8), 467-469.
- [2] Richard, H. A., Schramm, B., & Zipsner, T. (Eds.). (2017). *Additive Fertigung von Bauteilen und Strukturen*. Springer-Verlag.
- [3] Levy, G. N., Schindel, R., & Kruth, J. P. (2003). Rapid manufacturing and rapid tooling with layer manufacturing (LM) technologies, state of the art and future perspectives. *CIRP annals*, 52(2), 589-609.
- [4] Pascual, A., Ortega, N., Plaza, S., de Lacalle, L. N. L., & Ukar, E. (2023). Analysis of the influence of L-PBF porosity on the mechanical behavior of AlSi10Mg by XRCT-based FEM. *Journal of Materials Research and Technology*, 22, 958-981.
- [5] Lachmayer, R., Rettschlag, K., & Kaierle, S. (Eds.). (2021). *Konstruktion für die Additive Fertigung 2020*. Springer Vieweg.
- [6] Aboulkhair, N. T., Maskery, I., Tuck, C., Ashcroft, I., & Everitt, N. M. (2016). The microstructure and mechanical properties of selectively laser melted AlSi10Mg: The effect of a conventional T6-like heat treatment. *Materials Science and Engineering: A*, 667, 139-146.
- [7] Yang, C., Zhu, K., Liu, Y., Cai, Y., Liu, W., Zhang, K., & Huang, J. (2021). A comparative study of fatigue energy dissipation of additive manufactured and cast AlSi10Mg alloy. *Metals*, 11(8), 1274.
- [8] Bargel, H. J.; Schulze, G.: *Werkstoffkunde*, 12. Auflage, Berlin, Heidelberg, 2018, S. 501 – 502 DOI: 10.1007/978-3-662-48629-0
- [9] Sausto, F., Carrion, P. E., Shamsaei, N., & Beretta, S. (2022). Fatigue failure mechanisms for AlSi10Mg manufactured by L-PBF under axial and torsional loads: The role of defects and residual stresses. *International Journal of Fatigue*, 162, 106903.
- [10] Murakami, Y., Masuo, H., Tanaka, Y., & Nakatani, M. (2019). Defect analysis for additively manufactured materials in fatigue from the viewpoint of quality control and statistics of extremes. *Procedia Structural Integrity*, 19, 113-122.
- [11] Macias, J. G. S., Elangeswaran, C., Zhao, L., Buffière, J. Y., Van Hooreweder, B., & Simar, A. (2021). Fatigue crack nucleation and growth in laser powder bed fusion AlSi10Mg under as built and post-treated conditions. *Materials & Design*, 210, 110084.
- [12] Caivano, R., Tridello, A., Chiandussi, G., Qian, G., Paolino, D., & Berto, F. (2021). Very high cycle fatigue (VHCF) response of additively manufactured materials: A review. *Fatigue & Fracture of Engineering Materials & Structures*, 44(11), 2919-2943.
- [13] Schulze, V., Gibmeier, J., & Kacaras, A. (2017). Qualification of the stream finishing process for surface modification. *CIRP Annals*, 66(1), 523-526.
- [14] Zanger, F., Kacaras, A., Neuenfeldt, P., & Schulze, V. (2019). Optimization of the stream finishing process for mechanical surface treatment by numerical and experimental process analysis. *CIRP Annals*, 68(1), 373-376.
- [15] Kacaras, A., Gibmeier, J., Zanger, F., & Schulze, V. (2018). Influence of rotational speed on surface states after stream finishing. *Procedia CIRP*, 71, 221-226.
- [16] Hashimoto, F., & DeBra, D. B. (1996). Modelling and optimization of vibratory finishing process. *CIRP annals*, 45(1), 303-306.
- [17] Calignano, F., Manfredi, D., Ambrosio, E. P., Iuliano, L., & Fino, P. (2013). Influence of process parameters on surface roughness of aluminum parts produced by DMLS. *The International Journal of Advanced Manufacturing Technology*, 67, 2743-2751.
- [18] Uhlmann, E., Fleck, C., Gerlitzky, G., & Faltin, F. (2017). Dynamical fatigue behavior of additive manufactured products for a fundamental life cycle approach. *Procedia CIRP*, 61, 588-593.
- [19] Radaj, Dieter & Vormwald, Michael. (2007). *Ermüdungsfestigkeit: Grundlagen für Ingenieure*. 10.1007/978-3-540-71459-0.
- [20] Zimmermann, M., Müller, D., Kirsch, B., Greco, S., & Aurich, J. C. (2021). Analysis of the machinability when milling AlSi10Mg additively manufactured via laser-based powder bed fusion. *The International Journal of Advanced Manufacturing Technology*, 112, 989-1005.
- [21] Bagherifard, S., Beretta, N., Monti, S., Riccio, M., Bandini, M., & Guagliano, M. (2018). On the fatigue strength enhancement of additive manufactured AlSi10Mg parts by mechanical and thermal post-processing. *Materials & Design*, 145, 28-4